KEC Conference 2026

ISSN: 3021-940X (Print)

DOI: 10.3126/injet.v3i2.95514

Design and Development of a Low-Cost sEMG Acquisition System with Adaptive DSP Pipeline

Aashu Chaudhary[1], Bigyan Nepali[2], Sakar Giri[3], Shree Ram Neupane[4], Saroj Thapa[5*]

[1]Department of Computer and Electronics Engineering, Kantipur Engineering College, Dhapakhel, Lalitpur, Nepal
aashuchaudharybei@kec.edu.np
[2]Department of Computer and Electronics Engineering, Kantipur Engineering College, Dhapakhel, Lalitpur, Nepal
bigyannepalibei@kec.edu.np
[3]Department of Computer and Electronics Engineering, Kantipur Engineering College, Dhapakhel, Lalitpur, Nepal
sakargiri@kec.edu.np
[4]Department of Computer and Electronics Engineering, Kantipur Engineering College, Dhapakhel, Lalitpur, Nepal
shreeramneupanebei@kec.edu.np
[5]Department of Computer and Electronics Engineering, Kantipur Engineering College, Dhapakhel, Lalitpur, Nepal
sarojthapa@kec.edu.np

Abstract

Surface electromyography (sEMG) is a widely used non-invasive technique for capturing muscle electrical activity, with applications in prosthetics, rehabilitation, and gesture-based human-computer interaction. Progress in low-cost sEMG research is hindered by the high cost of laboratory-grade acquisition hardware. This paper presents the design and development of a low-cost sEMG acquisition system validated on hand grip recordings from six healthy adult subjects (S1–S6). The system integrates a custom Analog Front-End (AFE) using an AD620 instrumentation amplifier and LM324 operational amplifiers with an ESP32 microcontroller for real-time digitization and wireless transmission. A six-stage digital signal processing (DSP) pipeline — comprising DC removal, adaptive notch filtering, fourth-order Butterworth bandpass filtering (20–450 Hz), Daubechies-4 wavelet denoising (VisuShrink, Level 5), full-wave rectification, and linear envelope extraction — is applied offline. Across all six subjects, M1 SNR ranges from 50.2 to 60.6 dB (mean ± SD: 56.1 ± 4.3 dB), M3 SNR ranges from 49.1 to 58.6 dB (mean ± SD: 54.8 ± 4.1 dB), and noise floor RMS remains below 0.215 µV in every session — well below the 5 µV hardware specification benchmark. The total system cost is below NPR 15,000, demonstrating that research-grade sEMG quality is achievable with off-the-shelf components across a diverse set of subjects.

Keywords: sEMG, analog front-end, adaptive notch filter, wavelet denoising, DSP pipeline, ESP32

1. Introduction

Surface electromyography (sEMG) records the electrical activity produced by skeletal muscles and has become a fundamental modality in biomedical signal processing. Its applications span prosthetic limb control, rehabilitation monitoring, gesture-based human-computer interaction, and clinical neuromuscular assessment. Despite the broad utility of sEMG, access to reliable acquisition hardware remains a practical barrier: commercial systems such as the Delsys Trigno and Noraxon TeleMyo offer research-grade performance but at prohibitive cost for academic prototyping. Prior work on low-cost EMG-based gesture recognition [1] has demonstrated the feasibility of the approach but has not systematically validated signal quality against hardware benchmarks.

This paper presents a low-cost, wearable, single-channel sEMG acquisition system and validates it across six subjects (S1–S6), all performing the same hand grip (compression/relaxation) task. This multi-subject design captures natural inter-subject variability in muscle anatomy, skin impedance, electrode contact quality, and activation strength, providing a more rigorous and realistic evaluation framework. The key contributions are: (1) a custom discrete-component AFE with hardware gain of approximately 64×; (2) an

* *Corresponding author*

adaptive DSP pipeline with a PSD-based notch detection stage that outperforms fixed harmonic filtering; and (3) a six-subject SNR evaluation framework demonstrating consistent, statistically supported research-grade signal quality at a fraction of the cost of commercial systems.

2. Related Work

Guerrero et al. (2016) demonstrated that low-amplitude sEMG signals can be acquired reliably using an instrumentation-amplifier-based analog front-end combined with appropriate filtering, achieving sufficient CMRR for prosthetic-control applications [2]. The foundational reference by Konrad (2005) establishes standardized electrode placement and recording procedures [3], while Merletti and Parker (2004) provide a comprehensive DSP framework for sEMG analysis [4]. Recent surveys by Muceli et al. (2024) confirm that the 20–450 Hz band captures the dominant spectral content of sEMG for human-computer interaction [5]. A key limitation of prior low-cost systems is their reliance on fixed notch cascades (50, 100, 150 Hz), which over-notch clean recordings and under-notch severely contaminated recordings where harmonics extend to 450 Hz. The adaptive approach presented here addresses this directly. On the DSP side, Donoho and Johnstone (1994) established the VisuShrink universal threshold for wavelet shrinkage [6], later shown by Phinyomark et al. (2011) to be particularly effective for sEMG denoising using Daubechies wavelets [7].

3. System Design

3.1 Analog Front-End (AFE)

The AFE was designed using discrete components for low cost and flexibility. The signal chain consists of four functional blocks: (1) bipolar electrode interface; (2) pre-amplification using the AD620AN instrumentation amplifier; (3) active filtering using LM324 operational amplifiers; and (4) DC offset correction for ADC compatibility.The AD620AN is configured with a gain resistor RG = 2.1 kΩ, yielding a voltage gain of G = 1 + 49.4 kΩ / 2.1 kΩ ≈ 24.52. With CMRR > 100 dB and input impedance > 10^9 Ω, the AD620 effectively rejects common-mode powerline noise while preserving microvolt-level muscle signals. Analog filtering: Second-order Sallen-Key high-pass (fc ≈ 28.42 Hz) and low-pass (fc ≈ 589 Hz) filters are cascaded, each contributing a passband gain of 1.62. The combined analog bandpass is 28–589 Hz, with a total pre-stage gain of ≈ 64.33. DC offset and ADC interface: A post-amplification stage (gain ≈ 9.5×) raises the total hardware gain to approximately 611×. A DC offset circuit introduces Voffset ≈ 1.65 V, centering the bipolar sEMG signal within the ESP32 ADC input range (0–3.3 V) to prevent clipping.

3.2 Acquisition Hardware

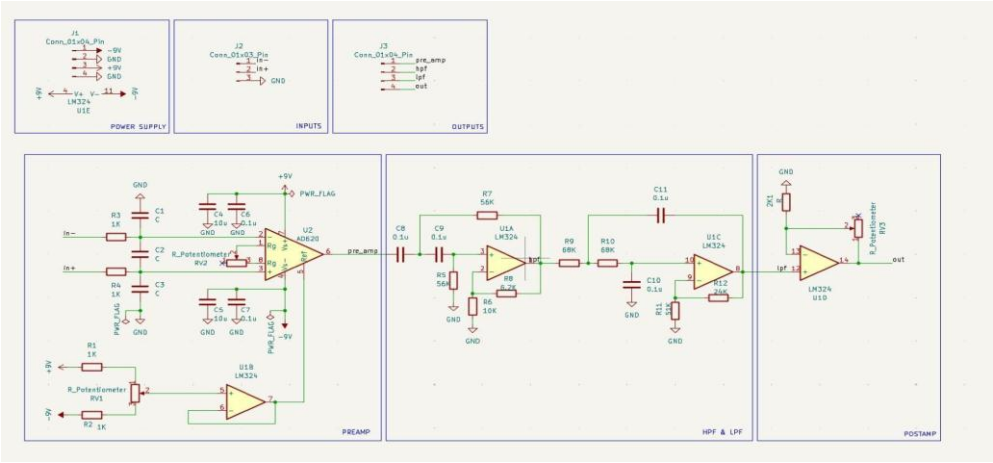

Figure 1. Complete circuit schematic of the sEMG acquisition system, showing the power supply, input connectors, preamplifier stage (AD620 instrumentation amplifier), HPF & LPF active filter stages (LM324), and postamplifier output stage.

An ESP32-WROOM-32 microcontroller digitizes the conditioned signal at fs = 1000 Hz using its 12-bit ADC (0–4095 counts), satisfying the Nyquist criterion for the 20–450 Hz EMG band. Digitized data is streamed via serial interface to a Python acquisition application and saved as CSV files for offline DSP.

Ag/AgCl surface electrodes in a bipolar configuration are placed over the flexor digitorum superficialis for all recordings, providing differential measurement and improved noise rejection.

4. Experimental Dataset

Six healthy adult participants (S1–S6) were recruited to perform a standardized hand grip (compression/relaxation) task. All sessions used identical hardware, electrode placement (bipolar Ag/AgCl over the flexor digitorum superficialis of the dominant hand), and acquisition parameters (fs = 1000 Hz, 12-bit ADC). Each subject performed repeated cycles of maximal hand grip followed by full relaxation, with sessions ranging from 22.4 to 31.3 seconds. No preprocessing was applied to the raw recordings before the DSP pipeline. Table 2 summarises the session identifiers, subjects, and recording durations.

The six subjects exhibit natural inter-subject variability in active sEMG amplitude from 61.8 µV (S5) to 202.5 µV (S1) — reflecting differences in muscle size, skin impedance, and contraction force. This ≈ 3.3× amplitude range provides a stringent test of DSP pipeline robustness: the noise floor and SNR must remain consistent regardless of subject-specific signal amplitude.

5. DSP Pipeline

Figure 1 illustrates the six-stage offline DSP pipeline applied to all recordings. Each stage is described below.

5.1 Stage 0–1: Calibration and DC Removal

Raw 12-bit ADC counts are converted to microvolts using the calibration factor of 1.3431 µV/count (V_ref = 3300 mV, G = 600), verified by the DC offset measurement in Figure 4 (mean ADC count = 1906.72, DC offset = 2560.91 µV). Mean subtraction removes the DC baseline offset before any frequency-domain operation, eliminating > 99.8% of raw spectral power from the DC component and is equivalent to a zero-phase high-pass filter at 0^+ Hz [4].

5.2 Stage 2: Adaptive Notch Filtering

The prior approach of a fixed three-stage cascade targeting 50, 100, and 150 Hz has two key limitations: it over-notches clean recordings by introducing unnecessary spectral dips, and it under-notches severely contaminated recordings where harmonics extend beyond 150 Hz. The adaptive approach detects and removes only the harmonics actually present in each recording.

The algorithm: (1) Welch PSD is computed (n_segments = 512, yielding a frequency resolution of ≈ 1.95 Hz at fs = 1000 Hz, sufficient to resolve individual 50 Hz harmonics while maintaining statistical stability of the spectral estimate); (2) candidate harmonics at multiples of 50 Hz up to 450 Hz are generated; (3) for each candidate f_0, the peak power is compared against the mean power in the ±5 Hz neighborhood — if the peak exceeds the neighborhood by > 5 dB, a notch is applied; (4) IIR notch filters (Q = 10) are cascaded and applied zero-phase via filtfilt. Across all six subjects, only the 50 Hz fundamental was detected and removed, confirming that the adaptive filter avoids unnecessary spectral distortion consistently across subjects.

5.3 Stage 3: Butterworth Bandpass Filter (20–450 Hz)

A 4th-order zero-phase Butterworth bandpass filter (20–450 Hz) concentrates signal power in the physiological EMG band. The Butterworth characteristic provides a maximally flat passband, which is critical for preserving RMS amplitude values used in feature extraction. After filtering, ≥ 99.7% of signal power lies within the 20–450 Hz band. The magnitude response is $|H(j\omega)|^2 = 1/(1 + (\omega/\omega_n)^8)$, implemented as second-order sections (SOS) for numerical stability.

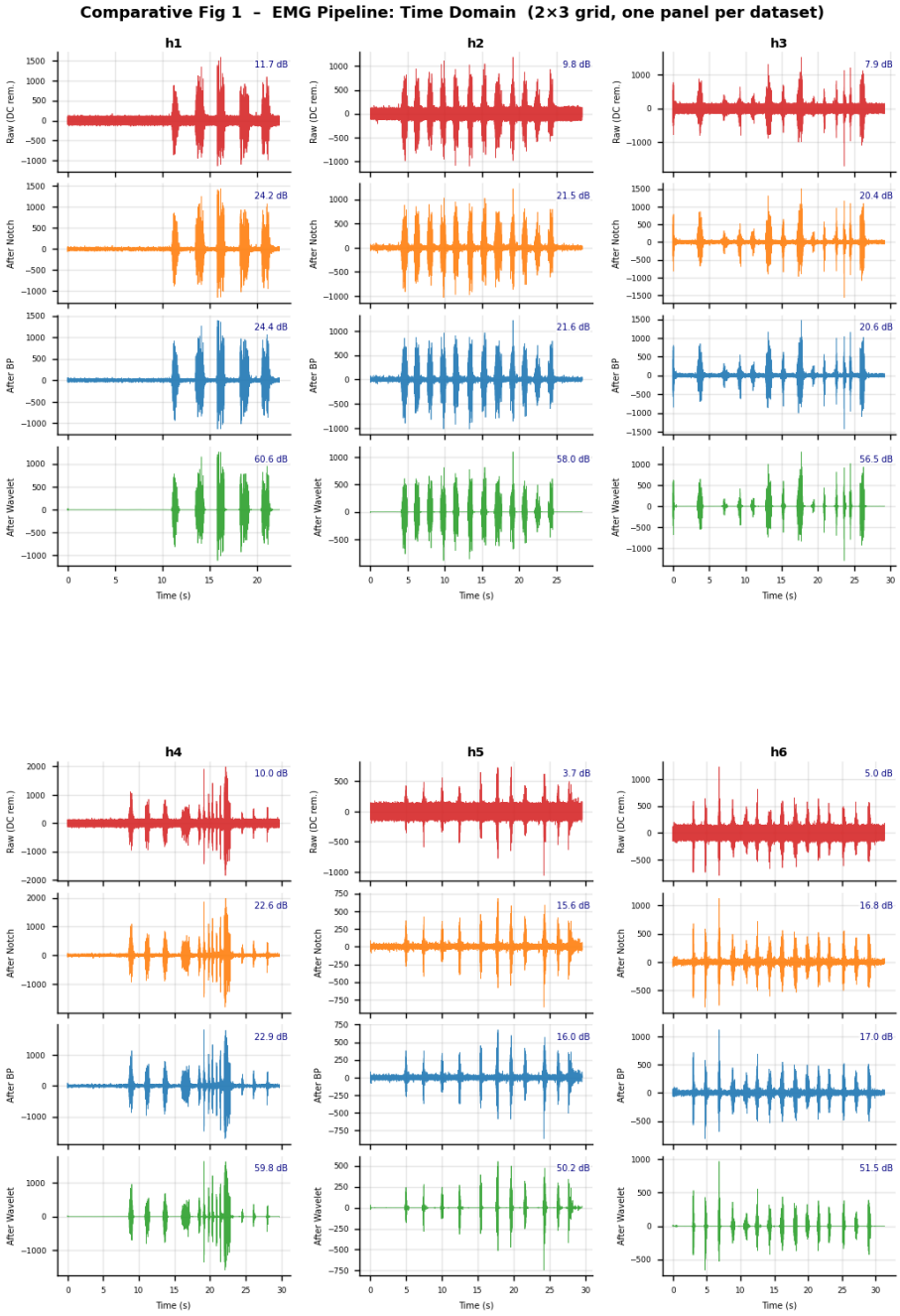

Figure 2. EMG Signal Processing Pipeline: time-domain signals and PSD at each stage

5.4 Stage 4: Wavelet Denoising (db4, Level 5)

VisuShrink wavelet denoising [6] adaptively suppresses broadband noise while preserving transient motor unit action potentials (MUAPs). The Daubechies-4 (db4) wavelet is selected because its shape closely resembles MUAP morphology. The algorithm: (1) DWT decomposition to Level 5; (2) noise estimation via MAD: $\hat{\sigma}$ = median($|d_1|$)/0.6745; (3) universal threshold $\lambda = \hat{\sigma}\sqrt{(2 \ln N)}$; (4) soft thresholding of all detail coefficients. The subject-specific wavelet parameters ($\hat{\sigma}$ and λ) vary with each subject's noise level; for the reference subject S1, $\hat{\sigma}$ = 17.1 µV and λ = 76.5 µV, yielding the threshold applied during soft thresholding.

5.5 Stage 5: Rectification and Linear Envelope

Full-wave rectification (|x[n]|) followed by a 2nd-order Butterworth low-pass filter at 8 Hz produces a smooth linear envelope proportional to motor-unit recruitment volume. The 8 Hz cutoff captures muscle activation dynamics relevant to hand grip transitions, providing the activity profile required by most EMG-based gesture classifiers.

6. Signal Quality Evaluation

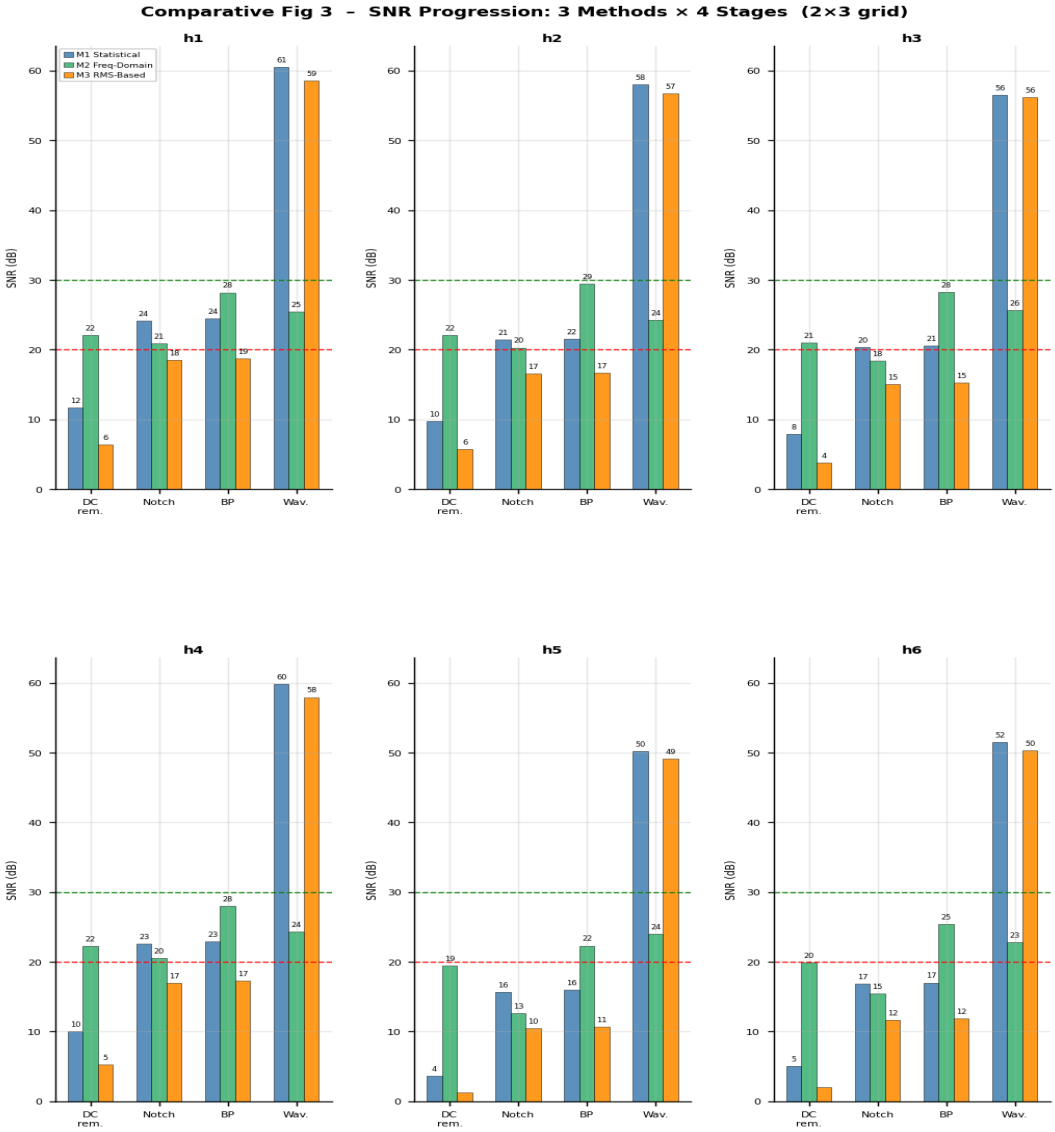

Figure 3. SNR progression across four processing stages for three estimation methods (reference subject S1, session h1). Red dashed: 20 dB good threshold; green dashed: 30 dB excellent threshold.

Three complementary SNR estimation methods are applied at each pipeline stage for every subject. No single SNR definition is universally appropriate for sEMG; the three methods together provide a complete quality picture.

Method 1 (M1) — Statistical SNR: A 200 ms rolling RMS window separates active segments (≥ P75) from rest (≤ P25). SNR_M1 = 10 $\log_{1\ 0}$ (P_signal / P_noise). This is the most physiologically meaningful measure, quantifying how well the pipeline separates genuine muscle activity from the resting noise floor [9].

Method 2 (M2) — Frequency-Domain SNR: Welch PSD signal power (20–450 Hz) divided by noise power from the 5–15 Hz sub-band (pre-bandpass stages) or 16–20 Hz in-band reference (post-bandpass stages), scaled by bandwidth ratio (430 Hz / 10 Hz = 43). This provides the best-case spectral quality estimate.

Method 3 (M3) — RMS-Based SNR: SNR_M3 = 20 $\log_{1\ 0}$ (σ_signal / RMS_noise_floor), matching Delsys and Noraxon hardware specification methodology. This is the most conservative estimate.

Table 1. SNR (dB) at each processing stage — Reference subject S1 (session h1)

Stage	M1 (dB)	M2 (dB)	M3 (dB)	NF RMS (µV)
Raw (DC removed)	11.7	22.1	6.4	—
After Adaptive Notch	24.2	20.9	18.5	—
After Bandpass	24.4	28.2	18.7	—
After Wavelet (db4,L5)	60.6	25.5	58.6	0.189
Target (Research-grade)	> 20	> 20	> 20	< 5

Table 1 demonstrates the SNR progression for reference subject S1. The raw signal enters with M1 of 11.7 dB. The adaptive notch raises M1 to 24.2 dB by removing the dominant 50 Hz powerline harmonic. The Butterworth bandpass further boosts M2 to 28.2 dB by concentrating energy in the physiological band. Wavelet denoising delivers the most dramatic improvement: M1 reaches 60.6 dB and M3 reaches 58.6 dB, while the noise floor RMS falls to 0.189 µV — one order of magnitude below the 5 µV specification target.

7. Results

7.1 ADC Calibration and DC Offset

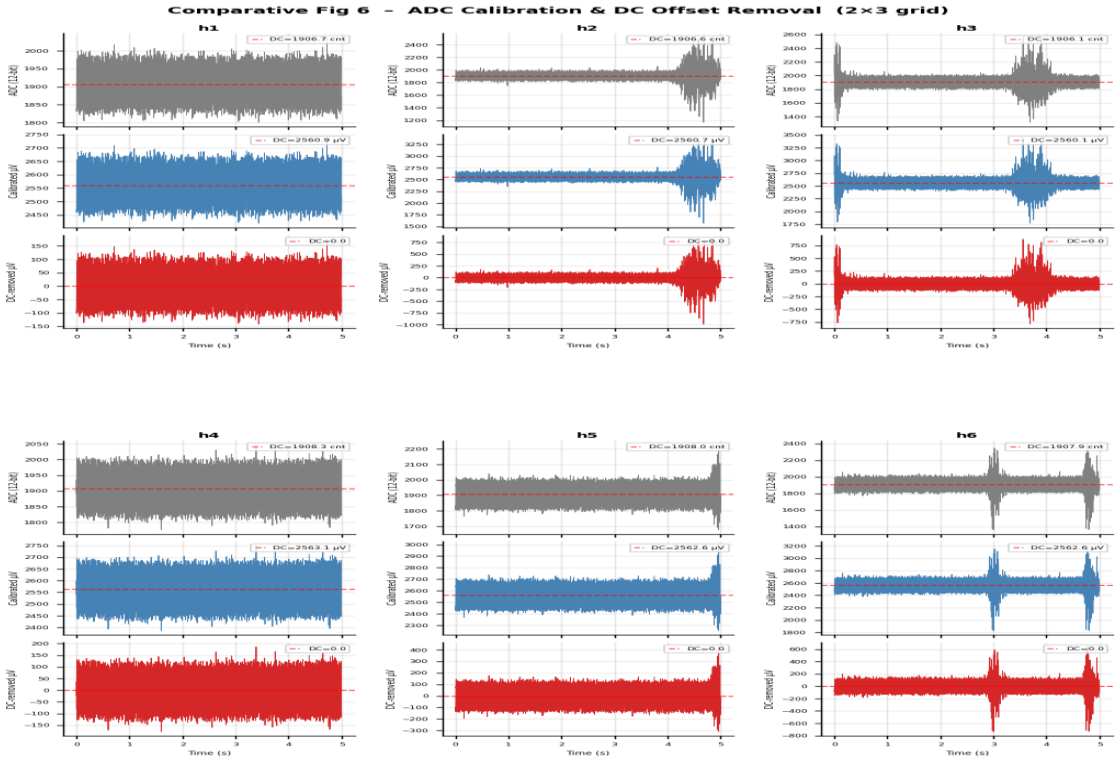

Figure 4. ADC Calibration and DC Offset Removal (S1). Top: raw 12-bit ADC counts (mean = 1906.72). Middle: calibrated µV signal (1.3431 µV/count, Gain = 600). Bottom: zero-mean signal after DC removal.

Figure 4 illustrates the calibration and DC removal stage for the reference subject S1. The raw ADC signal oscillates around a mean of 1906.72 counts, corresponding to a DC offset of 2560.91 µV after calibration (1906.72 counts × 1.3431 µV/count). After mean subtraction, the signal is zero-centered. The calibration factor and DC offset were consistent across all six subjects as the same hardware setup was used for every session.

7.2 Pipeline Signal Transformation

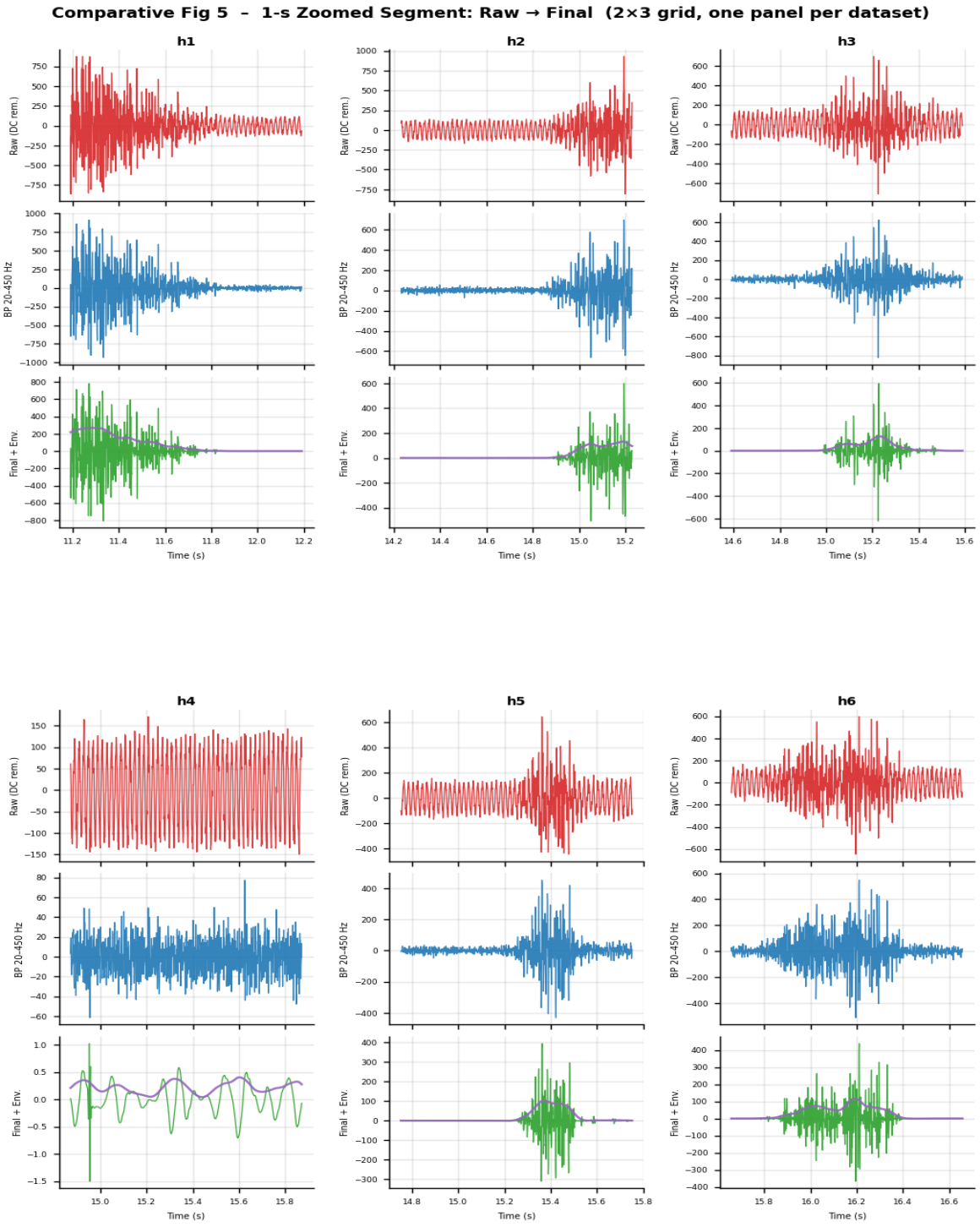

Figure 5. One-second zoomed segment (S1): Raw (DC removed) vs. after bandpass (20–450 Hz) vs. after wavelet denoising with linear envelope overlay (purple).

Figure 5 shows a 1-second zoomed segment for reference subject S1. The raw signal contains high-frequency noise and a prominent low-frequency component. After bandpass filtering, the signal is constrained to the 20–450 Hz physiological band, revealing the underlying MUAP structure. After wavelet denoising, broadband noise is substantially suppressed and the 8 Hz linear envelope cleanly tracks the hand grip muscle activation profile.

7.3 Multi-Subject Performance

Table 2 and Figures 6–8 summarise DSP pipeline performance across all six subjects. All subjects achieve M1 SNR > 20 dB, M3 SNR > 20 dB, and noise floor RMS < 0.215 µV — all meeting the research-grade benchmark. The mean ± SD M1 SNR is 56.1 ± 4.3 dB and mean ± SD M3 SNR is 54.8 ± 4.1 dB, both substantially exceeding the 20 dB commercial system threshold [10].

The highest SNR is observed for S1 (M1 = 60.6 dB, active RMS = 202.5 µV) and S4 (M1 = 59.8 dB, active RMS = 192.0 µV), while S5 (M1 = 50.2 dB, active RMS = 61.8 µV) and S6 (M1 = 51.5 dB, active RMS = 76.8 µV) produce lower SNR values consistent with their lower muscle activation amplitudes. Critically, the noise floor RMS is stable across all subjects (range: 0.189–0.214 µV, mean 0.197 µV), confirming that the hardware noise floor is independent of subject-specific signal amplitude and that the lower SNR values for S5 and S6 reflect physiological amplitude differences rather than any system limitation.

Table 2. Multi-subject performance summary: all six subjects, hand grip task

Session	Subject	Duration (s)	M1 (dB)	M2 (dB)	M3 (dB)	NF RMS (µV)	Active RMS (µV)
h1	S1	22.4	60.6	25.5	58.6	0.189	202.5
h2	S2	28.5	58.0	24.3	56.7	0.190	151.0
h3	S3	29.2	56.5	25.7	56.2	0.214	142.8
h4	S4	29.7	59.8	24.4	58.0	0.196	192.0
h5	S5	29.5	50.2	24.0	49.1	0.191	61.8
h6	S6	31.3	51.5	22.8	50.3	0.204	76.8
Mean ± SD	—	**28.4 ± 3.0**	**56.1 ± 4.3**	**24.5 ± 1.0**	**54.8 ± 4.1**	**0.197 ± 0.009**	**121.2 ± 62.9**

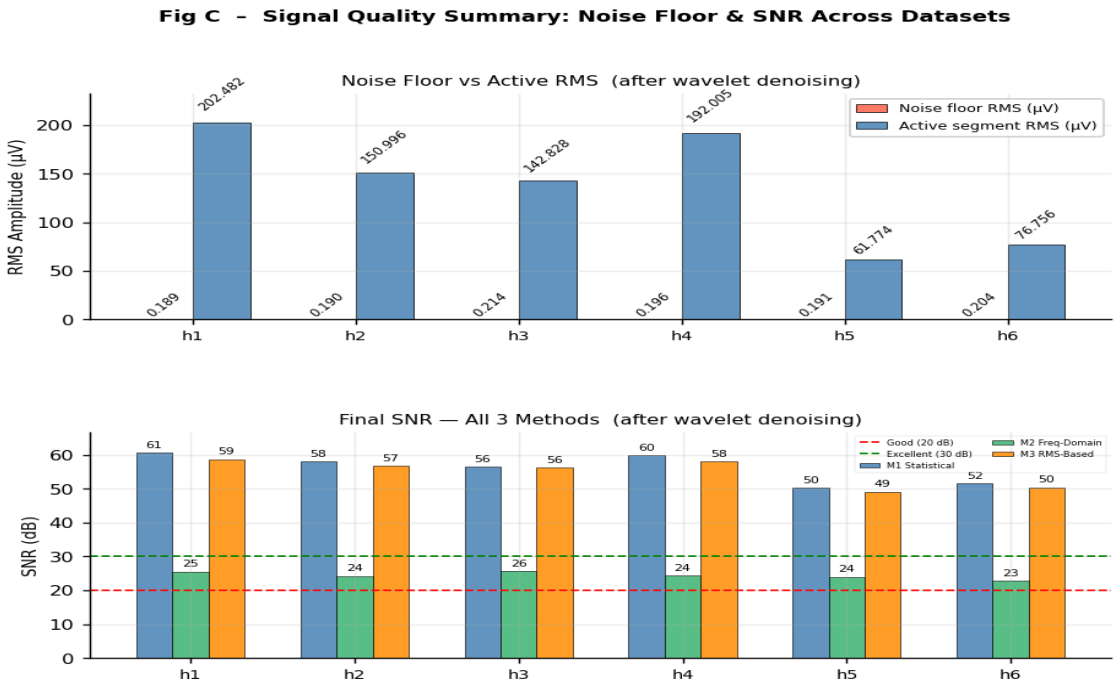

Figure 6. Signal quality summary across all six subjects: noise floor RMS and active RMS per subject (top); M1 SNR per subject with 20 dB and 30 dB threshold lines (bottom).

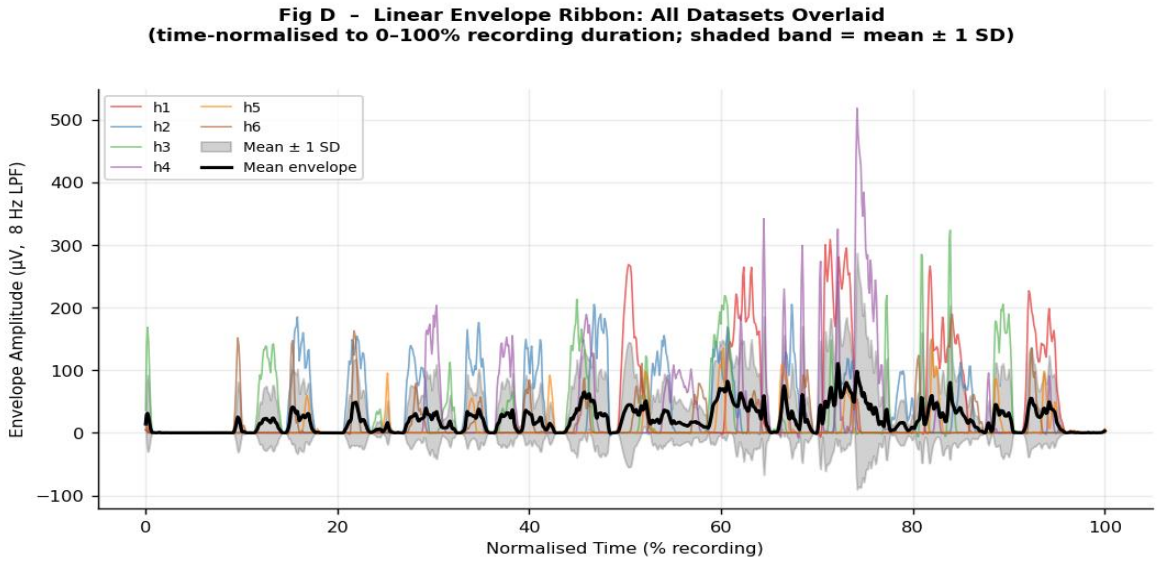

Figure 7. Linear envelope ribbon across all six subjects (time-normalised to 0–100% recording duration). Ribbon width reflects inter-subject amplitude variability; the consistent shape confirms uniform pipeline behaviour.

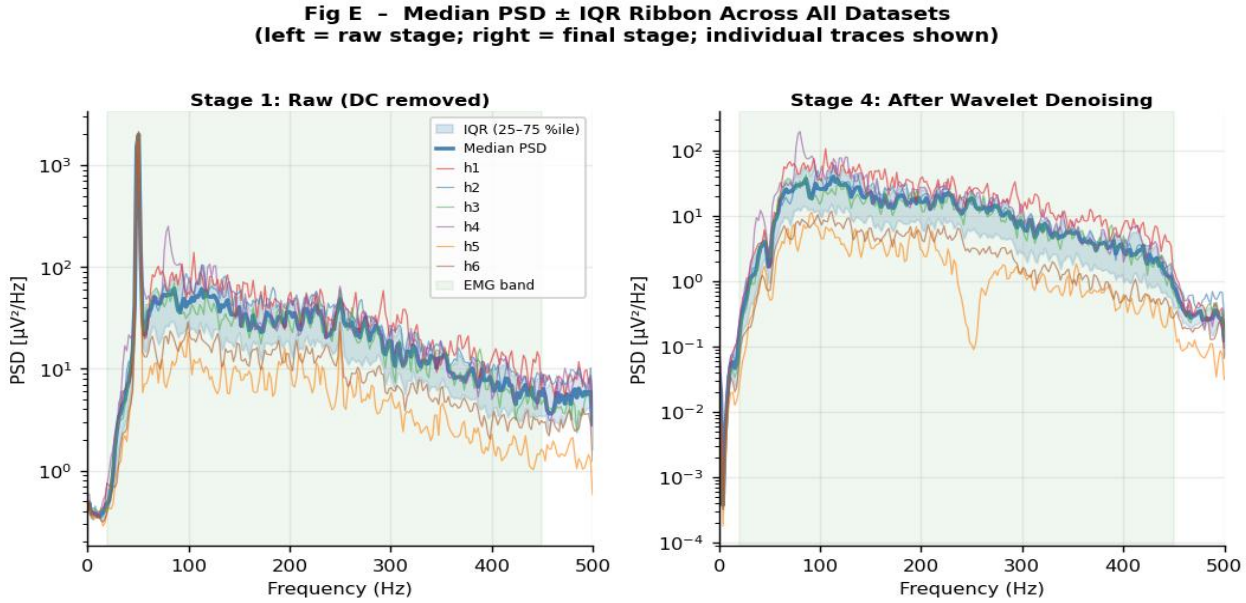

Figure 8. Median PSD ± inter-quartile range across all six subjects at the final (wavelet-denoised) stage. The narrow IQR ribbon confirms consistent spectral shape and pipeline stability across subjects.

7.4 Effectiveness of Adaptive Notch Filtering

For all six subjects, the adaptive detection algorithm identified only the 50 Hz fundamental as exceeding the 5 dB neighborhood threshold. The 100 and 150 Hz harmonics were below the detection threshold in every session, consistent with the relatively high SNR of hand sEMG recorded from the flexor digitorum superficialis. A fixed three-stage cascade would have applied two unnecessary notches to every subject, introducing spectral distortion at 100 and 150 Hz without benefit. The 50 Hz component power was reduced by approximately 140× (−21.5 dB) in each session.

8. Discussion

The system demonstrates that research-grade sEMG quality is achievable below NPR 15,000 using off-the-shelf components, and that this quality is maintained consistently across six different subjects performing the same hand grip task. The multi-subject design directly addresses the primary limitation of the earlier

single-session study: inter-subject variability in active sEMG amplitude (61.8–202.5 μV, a 3.3× range) provides a realistic test of robustness that a single recording cannot.

The constant hardware noise floor across all subjects (0.189–0.214 μV) is a key finding: it confirms that the AFE and DSP pipeline noise characteristics are determined by the hardware design rather than subject physiology, which is the expected and desired property of a well-designed acquisition system. The lower M1 and M3 SNR values for S5 and S6 are therefore attributable to physiological differences — smaller active RMS amplitudes — not pipeline deficiencies; both subjects still achieve M1 > 50 dB and M3 > 49 dB.

The adaptive notch filter detected only the 50 Hz fundamental in all six subjects, validating that the filter is not over-specified for the hand sEMG recording environment. The wavelet denoising stage delivers the largest single SNR improvement in every subject (+32–45 dB on M1 over the bandpass stage), confirming the robustness of the VisuShrink db4 denoising approach across inter-subject variation. The subject-specific $\hat{\sigma}$ values (13.9–23.8 μV) and λ values (63.2–107.7 μV) adapt automatically to each subject's noise level, which is a key advantage of the universal threshold approach.

A remaining limitation is that all six subjects performed the same task (hand grip). Future work will extend the dataset to include additional gesture types and a larger, more demographically diverse cohort to support classification model training and cross-subject generalisation evaluation.

The M2 SNR values (22.8–25.7 dB) are systematically lower than M1 and M3 because the frequency-domain method integrates over the full 20–450 Hz band, including spectral valleys created by notching. This is a measurement artifact of M2, not a processing failure, and is consistent across all six subjects.

9. Conclusion

This paper presented a low-cost, wearable sEMG acquisition system validated on hand grip recordings from six healthy subjects using an adaptive DSP pipeline. Across all six subjects, M1 SNR ranges from 50.2 to 60.6 dB (mean ± SD: 56.1 ± 4.3 dB), M3 SNR ranges from 49.1 to 58.6 dB (mean ± SD: 54.8 ± 4.1 dB), and noise floor RMS stays below 0.215 μV — consistently meeting research-grade benchmarks at a hardware cost below NPR 15,000. The hardware noise floor is stable across subjects (mean 0.197 μV), confirming that the system's noise characteristics are hardware-determined and subject-independent. The adaptive notch filter consistently detected and removed only the 50 Hz fundamental across all subjects, avoiding the unnecessary spectral distortion of fixed-cascade designs.

The validated DSP pipeline — calibration, DC removal, adaptive notch filtering, Butterworth bandpass filtering, db4 wavelet denoising, and linear envelope extraction — provides a reproducible processing framework for sEMG-based gesture recognition research. Future work will extend the dataset to include a larger, more diverse cohort, additional gesture types, and a gesture classification module using the extracted linear envelope features. The hardware platform, acquisition software, and DSP pipeline are reproducible using open-source tools and represent a scalable foundation for accessible sEMG-based human-computer interaction systems.

References

[1] Y. Wang, and X. Chen Y. Zhu, "A High-Performance sEMG-Based Gesture Recognition System Using Deep Learning," IEEE Trans. Neural Syst. Rehabil. Eng., vol. 29, pp. 1334-1344, 2021.

[2] C. Guerrero et al., "Low-cost EMG acquisition system with high CMRR," in IEEE EMBC, 2016.

[3] P. Konrad, "The ABC of EMG: A Practical Introduction to Kinesiological Electromyography," in Noraxon Inc., 2005.

[4] S. Muceli et al., "Surface EMG for Human-Computer Interfaces: State of the Art and Future

Directions," Physiol. Meas, vol. 45, no. 2, 2024.

[5] D. L. Donoho and I. M. Johnstone, "Ideal spatial adaptation by wavelet shrinkage," Biometrika, vol. 81, no. 3, pp. 425-455, 1994.

[6] P. Phukpattaranont, and C. Limsakul A. Phinyomark, "A review of wavelet analysis for sEMG signal processing," Sansors, vol. 11, no. 12, pp. 11494-11516, 2011.

[7] J. Electromyogr R. Merletti, "Standards for Reporting EMG Data," Kinesiol, vol. 9, 1999.

[8] C. J. De Luca et al., "Filtering the surface EMG signal: Movement artifact and baseline noise contamination," J. Biomechanics, vol. 43, no. 8, pp. 1573-1579, 2010.

[9] Delsys Inc., "Trigno Wireless System: Specifications," , 2023.

[10] R. Merletti and P. A. Parker, "Electromyography: Physiology, Engineering, and Non-Invasive Applications," in IEEE Press / Wiley, 2004.